Lawrence Berkeley National Laboratory

Title
Tuning Reactivity and Electronic Properties through Ligand Reorganization within a Cerium Heterobimetallic Framework

Permalink
https://escholarship.org/uc/item/1r45p0h7

Author
Robinson, Jerome R.

Publication Date
2013-12-18

DOI
10.1021/ja410688w

Peer reviewed

Tuning Reactivity and Electronic Properties through Ligand Reorganization within a Cerium Heterobimetallic Framework

Jerome R. Robinson,[a] Zachary Gordon,[a] Corwin H. Booth,[b] Patrick J. Carroll,[a] Patrick J. Walsh,[a]* and Eric J. Schelter[a]*

a – P. Roy and Diana T. Vagelos Laboratories, Department of Chemistry, University of Pennsylvania, Philadelphia, PA 19104, United States

b – Chemical Sciences Division, Lawrence Berkeley National Laboratory, Berkeley, CA 94720, United States

ABSTRACT: Cerium compounds have played vital roles in organic, inorganic, and materials chemistry due to their reversible redox chemistry between trivalent and tetravalent oxidation states. However, attempts to rationally access molecular cerium complexes in both oxidation states have been frustrated by unpredictable reactivity in cerium(III) oxidation chemistry. Such oxidation reactions are limited by steric saturation at the metal ion, which can result in high energy activation barriers for electron transfer. An alternative approach has been realized using a rare earth/alkali metal/1,1'–BINOLate (REMB) heterobimetallic framework, which uses redox-inactive metals within the secondary coordination sphere to control ligand reorganization. The rational synthesis of functionalized cerium(IV) products and a mechanistic examination of the role of ligand reorganization in cerium(III) oxidation are presented.

1. Introduction

Cerium is a lanthanide element of major importance because of its accessible $4f^1/4f^0$ redox couple,[1] which has been utilized in organic,[2] inorganic,[3] and materials chemistry.[4] In materials chemistry, cerium oxides and related ceria-zirconia solid solutions are widely used in oxidative and reductive applications including as heterogeneous catalysts in organic transformations,[5] three-way automotive catalytic converters,[4c-e,6] fuel cells,[7] and in the water gas-shift reaction.[8] Applications of cerium reagents in molecular chemistry have largely focused on the strong oxidizing potential of Ce^{IV} in electron deficient ligand frameworks,[1-3,3d-f] while the use of electron-rich frameworks to produce Ce^{III} reductants have received considerably less attention.[9] It is evident that the diverse application of cerium-based materials is not reflected by applications of its molecular compounds. In order to expand the chemistry of the $Ce^{III/IV}$ couple, and to isolate new molecular Ce^{IV} moieties, predictable and controlled redox behavior for molecular cerium compounds must be established.

Kinetic aspects, such as ligand reorganization, have been implicated in the unpredictable reactivity observed in the oxidation of Ce^{III} compounds.[1c,10] Reorganizational energy plays a central role in electron transfer; large reorganization energies contribute to significant activation barriers, which have important implications in biological,[11] organic,[12] and inorganic[13] redox properties and reactivity. While the impact of reorganization energy has been the subject of numerous studies, there have been limited reports pertaining to redox chemistry of the rare earth (RE) cations.[9a,14] This is surprising considering the predominantly ionic bonding observed in $4f$ systems.[1b,c] At $4f$ cations, coordination spheres are typically sterically saturated, which would be expected to contribute to large reorganization energies.

Recently, we disclosed initial results illustrating the role of ligand reorganization in a heterobimetallic framework: REMB, RE = Ce; M = Li, Na, K; B = (S)‑BINOLate (RE:M:B = 1:3:3). We found that the choice of redox-inactive metal, M, controlled the ligand reorganization, electrochemical properties, and chemical reactivity of the complexes.[9a] Our key finding was that the accessibility of the Ce^{III} cation to Lewis-base
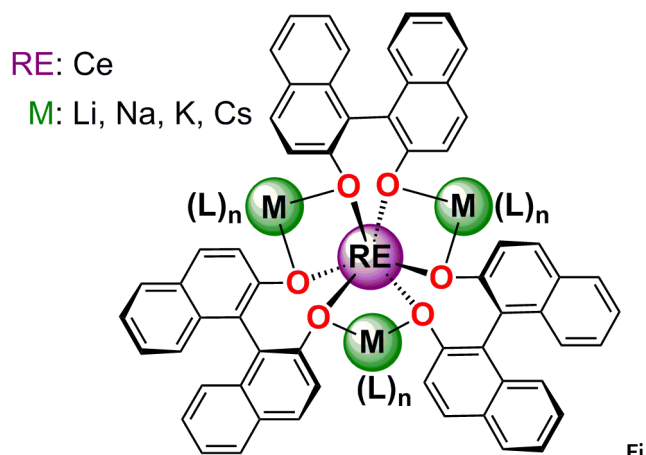

Figure 1. Shibasaki's REMB framework. RE = Rare Earths; M = Li, Na, K; B = (S) – BINOLate; RE:M:B = 1:3:3.

coordination, a direct reflection of ligand reorganization facilitated by the redox-inactive metal, dictated the rate of chemical oxidation and product outcome.

In the current work, we capitalize on our initial findings by demonstrating the broad oxidation chemistry of the cerium heterobimetallic system. For M = Li, the first general examples of inner sphere functionalization are achieved through complementary oxidative functionalization and salt-metathesis routes, while for M = Na, K, or Cs salt-eliminated products were observed. The family of functionalized Ce^{IV} complexes displays tunable electronic properties largely through choice of redox-inactive metal. Mechanistic insight is provided by chemical oxidation kinetics and isolation of model encounter complexes using triphenylphosphine oxide. Our experimental findings support an inner sphere oxidation mechanism predicated on the accessibility of the cerium cation (ligand reorganization), which is controlled by the identity of the redox-inactive metal.

2. Results and Discussion
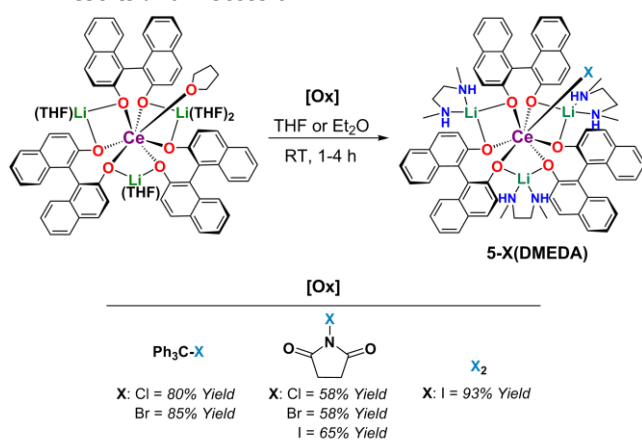
Scheme 1. Oxidative functionalization reactions of [Li$_3$(THF)$_4$][(BINOLate)$_3$Ce(THF)]·THF, **1.**

2.1 Synthesis and Characterization of Inner-sphere functionalized products (M = Li).

Inner-sphere Functionalization of [Li$_3$(THF)$_5$][(BINOLate)$_3$Ce·THF] (**1**) *with Chemical Oxidants*. The promise of using heterobimetallic frameworks for stabilizing cerium(IV) complexes was initially realized through study of the scope of the oxidation chemistry of [Li$_3$(THF)$_5$][(BINOLate)$_3$Ce·THF] (**1**). Whereas previous conditions for successful Ce^{III} oxidations have required judicious choice of ligand, solvent, and oxidant,[10a,15] oxidation reactions of **1** with trityl chloride did not display solvent dependence. The oxidation reaction of compound **1** with trityl chloride proceeded smoothly in coordinating (THF, DME) and non-coordinating (toluene, CH$_2$Cl$_2$) solvents to yield [Li$_3$(THF)$_5$][(BINOLate)$_3$Ce–Cl] (**2–Cl**) . Ligand substitution at the Li$^+$ cations did not result in different oxidation outcomes; oxidation of [Li$_3$(DMEDA)$_3$][(BINOLate)$_3$Ce] (**1–DMEDA**), or **1** followed by addition of 3 equiv of DMEDA to the crude oxidation mixture provided [Li$_3$(DMEDA)$_3$][(BINOLate)$_3$Ce–Cl]·C$_5$H$_{12}$, **2–Cl(DMEDA)** in 80% yield (Figure S34). Furthermore, the use of a different trityl halide, namely, trityl bromide, allowed for the isolation of the

[Li$_3$(DMEDA)$_3$][(BINOLate)$_3$Ce–Br], **2–Br(DMEDA)**, in 85% yield (Figure S35).

Recent work has emphasized that the choice of oxidant is critical to successful cerium oxidation reactions,[10b,15d,e] which prompted us to expand the oxidative chemistry of **1**. Using the measured $E_{1/2}$ value of **1** as a guide, E_{pa} = – 0.45 V *vs* Fc in THF, we expected that *N*-bromosuccinimide E_{pc} = –0.37 V *vs* Fc in CH$_3$CN,[16] and iodine, E_{pc} = –0.140 V *vs* Fc in CH$_3$CN,[17] could serve as mild oxidants. Treatment of **1** or **1–(DMEDA)** with 1 equiv of *N*-halosuccinimide reagents (NXS; X = Cl, Br, I) or 0.5 equiv of iodine proceeded smoothly to Ce^{IV} products.

Upon work up and crystallization from concentrated solutions of THF layered with pentane, [Li$_3$(DMEDA)$_3$][(BINOLate)$_3$Ce–X], **2–X(DMEDA)** (X = Cl, Br, I) were obtained in 58–93% crystalline yield (Scheme 1). The oxidative functionalization of **1** is not limited to the transfer of halides. We previously reported the reaction of **1** with 0.5 equiv of 1,4-benzoquinone, BQ, which afforded the tetravalent dimer, [{[Li$_3$(Et$_2$O)$_{3.5}$][(BINOLate)$_3$Ce]}$_2$(μ-O$_2$C$_6$H$_4$)]·Et$_2$O, **2–BQ**, in 89% yield.[9b] The importance of these results is that the cerium(III) oxidation reactions are general for **1** using various oxidants and solvents, which is a major advance in the molecular chemistry of cerium.

Single crystal X-ray data for oxidation products (X = Cl, Br, I) reveal seven coordinate Ce^{IV} ions in distorted face-capped octahedral geometries (Figure 5a). Few examples of terminal Ce^{IV}–halides have been reported.[10a,15a,15c,15e,18] The complexes **2–X(DMEDA)** X = Br, I represent only the third and second structurally characterized cerium(IV) bromide and iodide complexes, respectively. Overall, the complexes **2–X(DMEDA)** represent the first isostructural series of cerium complexes comprising Cl, Br, and I. The Ce^{IV}–X bond distances within the series increase according to the ionic radii of halide (I$^-$ > Br$^-$ > Cl$^-$), supporting the ionic nature of the Ce^{IV}–X bond (Table 2).

Scott and coworkers observed that the conformationally constrained tripodal amide framework, tren, forms dimeric class I mixed-valence oxidation products with more Lewis-basic halides (Cl$^-$, Br$^-$); however, this behavior was not observed for **1**. Furthermore, while I$_2$ and BQ could behave as inner or outer sphere oxidants,[19] reactions with **1** only produced inner sphere functionalized products.
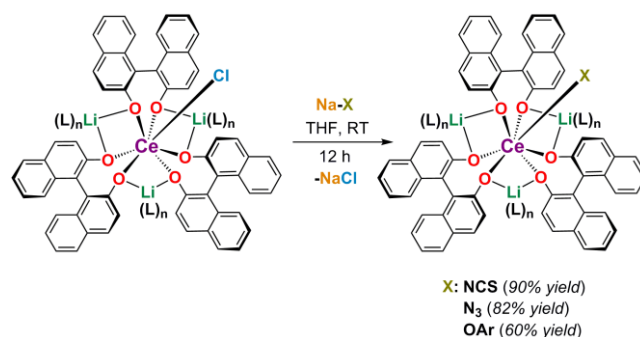
Scheme 2. Salt metathesis reactions of [Li$_3$(THF)$_5$][(BINOLate)$_3$Ce–Cl]·THF, **2–Cl**.
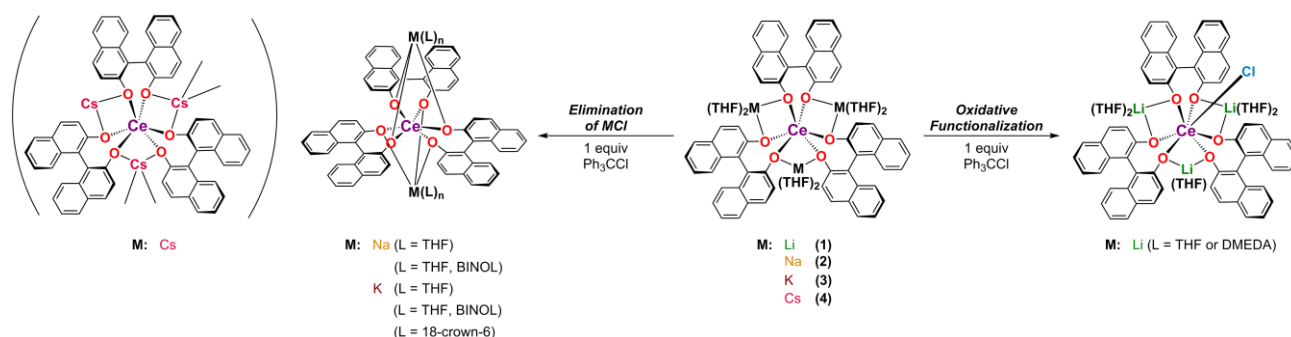
Scheme 3. Oxidative functionalization (right) and salt elimination (left) reaction pathways of CeMB.

Inner-sphere Functionalization Through Salt Metathesis. Although oxidative functionalization of **1** was successful compared to other cerium systems, this synthetic strategy is limited to 1 e⁻ group-transfer oxidants. To further demonstrate the utility of the Ce/Li platform, we pursued functionalization through complementary salt metathesis routes. Access to cerium(IV) complexes from ceric ammonium nitrate (CAN) has been used to synthesize alkoxide,[20] aryloxide,[18] and acetylacetaonato[21] complexes. However, there are limited reports concerning metathesis from a Ce^{IV} halide.[22] Treatment of **2–Cl** in THF with the sodium salts of pseudohalides (SCN⁻ and N$_3$⁻) and an aryloxide (⁻OAr; Ar = 4–Ph) readily afforded the inner-sphere functionalized products by salt elimination of NaCl (Scheme 2). Na⁺ for Li⁺ exchange was not observed within the REMB framework, and is consistent with cation exchange preferences in the RE^{3+} systems.[23]

The first example of a Ce^{IV} thiocyanate, [Li$_3$(THF)$_5$][(BINOLate)$_3$Ce–NCS] (**2–NCS**), was obtained after a toluene extraction followed by crystallization from concentrated solutions of THF layered with pentane in 90% yield and displayed a single N=C stretch centered at 2038 cm⁻¹ (Figure 2b). [Li$_3$(THF)$_5$][(BINOLate)$_3$Ce–N$_3$] (**2–N$_3$**) and [Li$_3$(DME)$_3$][(BINOLate)$_3$Ce–OAr]·2DME (**2–OAr**) were isolated in a similar manner in 82 and 60% yield respectively,

where crystallization of **2–OAr** was accomplished from concentrated solutions in DME layered with hexanes (Figure 2c).

Bonding metrics of **2–NCS**, **2–N$_3$**, and **2–OAr** are displayed in Table 1 and Table S1. **2–NCS** and **2–N$_3$** are isostructural and crystallize with two unique molecules in the asymmetric unit. **2–NCS** is the first Ce^{IV}–NCS bond and the thiocyanate fragment is N-bound with Ce^{IV}–N bond distances of 2.414(4) and 2.421(3) Å. The Ce^{IV}–NCS bond distances match well to terminal Ce^{III}–NCS bond distances after accounting for differences in ionic radii.[24] The Ce^{IV}–N distances in **2–N$_3$** of 2.361(5) and 2.345(5) Å are similar to the only previously reported cerium(IV) azide complex.[22a] The Ce^{IV}–OAr bond distance of **2–OAr** is also in agreement with Ce^{IV} Schiff-base and calixarene frameworks.[18,22] Notably, Ce^{IV}–O$_{BINOLate}$ and Li–O$_{BINOLate}$ distances vary slightly to accommodate the different Ce–X species (X = Cl, Br, I, O$_2$C$_6$H$_4$, NCS, N$_3$, OAr, Table 1 and Table S1). We propose that the heterobimetallic framework provides a flexible, yet-defined coordination environment, which facilitates straightforward and general oxidation and metathesis chemistry in good yields.

2.2 Synthesis and Characterization of Salt-eliminated products (M = Na, K, Cs).

The reactivity of the cerium heterobimetallic framework can be controlled by choice of redox-inactive metal; while **1**
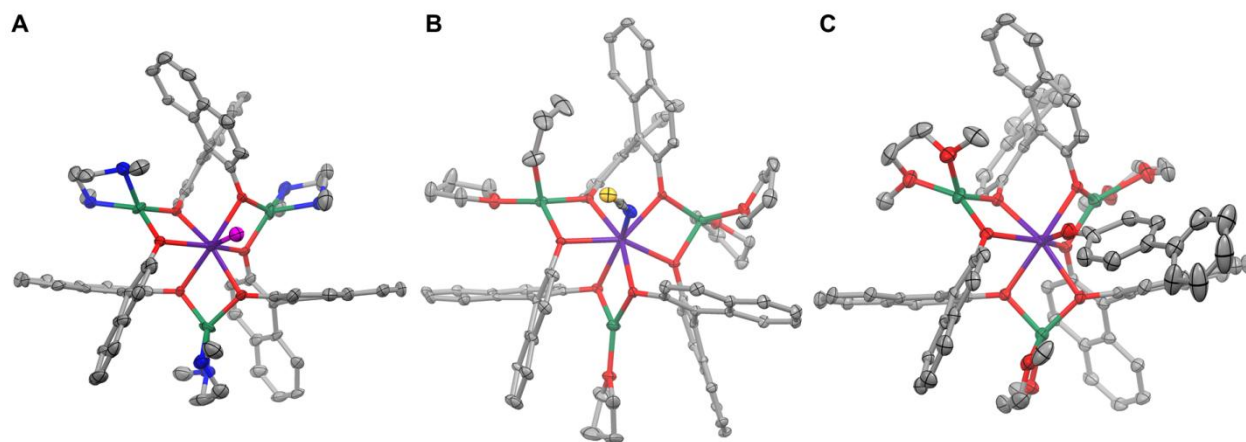
Figure 2. Thermal ellipsoid plots shown at 30% probability (A) [Li$_3$(DMEDA)$_3$][(BINOLate)$_3$Ce–I] (**2–I(DMEDA)**) (B) [Li$_3$(THF)$_5$][(BINOLate)$_3$Ce–NCS] (**2–NCS**) (C) [Li$_3$(DME)$_3$][(BINOLate)$_3$Ce–OAr] (**2–OAr**; Ar = 4–Ph)

readily undergoes oxidative functionalization, CeMB (M = Na (**3**), K (**5**)), undergo salt-elimination upon oxidation to form [M$_2$(THF)$_n$][(BINOLate)$_3$Ce] (M = Na (**4**), K (**6**)) in quantitative yield (Scheme 3).[9a] The preference for oxidative functionalization or salt-elimination follows the ability of the resulting cerium(IV) product to maintain a seven-coordinate geometry.

There have been no reports of other metal cations in the REMB framework outside of the lighter alkali metals (M = Li, Na, K). We, therefore, pursued the synthesis of a heavier alkali metal congener (M = Cs (**7**)). Synthesis of analytically pure CeCsB (**7**) was possible following an analogous protonolysis route used for the lighter alkali metals[9a] in 95% yield. Single crystals of **7** could be grown from layering concentrated THF solutions with pentane at −35° C; however, the structural data obtained from single crystal X-ray diffraction studies were only suitable to establish connectivity. A preliminary solution revealed **7** as a C_2 symmetric dimer in the solid state with the formula [Cs$_6$(THF)$_4$][(μ-BINOLate-κ-1O^1,2O^2)$_2$(BINOLate)$_4$Ce$_2$] (Figure S41). The cerium adopted a distorted trigonal prismatic geometry; the primary coordination sphere consisted of two chelated terminal BINOLate fragments per cerium center and two bridging BINOLate fragments, where the Cs$^+$ coordination environment is satisfied by Cs$^+$-π interactions from the BINOLate naphthyl carbons. Also, a displacement of the cerium center from the M$_3$ plane was negligible (0.018 Å) indicative of a relatively isolated Ce^{III} center that must undergo extensive reorganization in order to interact with solvent or substrate.[25]

Contrary to the C_2 symmetric dimer of **7** in the solid state, the dimer dissociates to two monomers in coordinating solvents. ^{1}H- and ^{13}C{^{1}H}-NMR in THF–d_8 were consistent with the expected D_3 solution symmetry observed for the lighter REMB complexes, while the DOSY NMR experimentally determined hydrodynamic radius (r_H) of **7** agreed best with a monomeric solution structure (see Supporting Information). Oxidation of **7** with trityl chloride proceeded to the salt-eliminated product that was isolated as the crystalline material, {[Cs$_2$][(BINOLate)$_3$Ce]·DME}$_∞$ (**8**) in 79% yield (Figure S42).

X-ray diffraction studies revealed considerable structural rearrangement in the salt-eliminated products. Crystallization of **4** and **6** with addition of different donor ligands, BINOL and 18–Crown–6, [M$_2$(THF)$_n$(BINOL)][(BINOLate)$_3$Ce] (M = Na (**4–BINOL**), K (**6–BINOL**)) and [K$_2$(18–Crown–6)$_2$][(BINOLate)$_3$Ce] (**6–Crown**) respectively, revealed a migration of M$^+$ to axially cap the tris(BINOLate) framework and collapse of the primary coordination sphere to a distorted octahedron (Scheme 3). Complex {[Cs$_2$][(BINOLate)$_3$Ce]·DME}$_∞$ (**8**) revealed another unique architecture for these Ce^{IV}-BINOLate frameworks (Figure S42). In the solid state, **8** was shown to be a coordination polymer. In this case, one Cs$^+$ cation bridges to another repeating unit through O$_{BINOLate}$–Cs and Cs$^+$–π interactions. The bridging interactions resulted in infinitely repeating helices, where one complete helical turn consisted of ~6 CeCsB units with a Ce–Ce separation of ~36 Å.

To the best of our knowledge, the Ce-BINOLate complexes represent the first system where the choice of redox-inactive metal (M$^+$) dictates whether selective oxidative functionalization or salt elimination occurs from the same ligand framework. Notably, the oxidation reactions of the heterobimetallic frameworks proceeded in high yields, and did not proceed by detrimental pathways such as ligand redistribution.[12b, 17b, 17d, 42] The modular reactivity of CeMB suggested that incorporation of redox-inactive metals can be an effective strategy for tuning reactivity and generating structural diversity within the same ligand framework. This is a particularly attractive attribute of the system, because lanthanide cations exhibit predominantly ionic bonding and large coordination numbers allowing for facile formation of alkali-metal "-ate" complexes.[26]

2.3 Electronic Properties of the Ce^{IV}MB Complexes

The electronic properties of Ce^{IV} complexes are of substantial interest to their redox applications hence, we set out to investigate the electronic properties of our family of structurally diverse Ce^{IV}-BINOLate heterobimetallic complexes.

X-ray Absorption Spectroscopy. Formally cerium(IV) complexes are known to exhibit valence ambiguity.[10a,27] Complexes **1**, **2–X(DMEDA)** (X = Cl, Br, I) and **2–BQ** were characterized through L_{III}-edge XAS to assign their oxidation states (Figure 4). As previously reported,[9b] complex **1** displays a single edge feature at 5725 eV that is consistent with a Ce^{III} oxidation state.[9b] The XAS data for **2–X(DMEDA)** (X = Cl, Br, I) support Ce^{IV} centers; the split features centered at ~5730 eV are typically observed for formal Ce^{IV} compounds,[28] and correspond to excitation of Ce^{IV} core electrons to final states $\overline{2p4f^1\underline{L}5d^1}$ and $\overline{2p4f^0 5d^1}$, where $\underline{L}$ indicates a ligand hole in this formalism). Similar behavior was also observed for **2–BQ**, where the two cerium centers were assigned as Ce^{IV} with no oxidation of the redox-active ligand, BQ$^{2−}$.[9b] The XAS data for **2–X(DMEDA)** support the assertion that the Ce^{IV} state is stabilized by the CeMB framework, and that no valence ambiguity occurs due to differences in halide nucleophilicity.
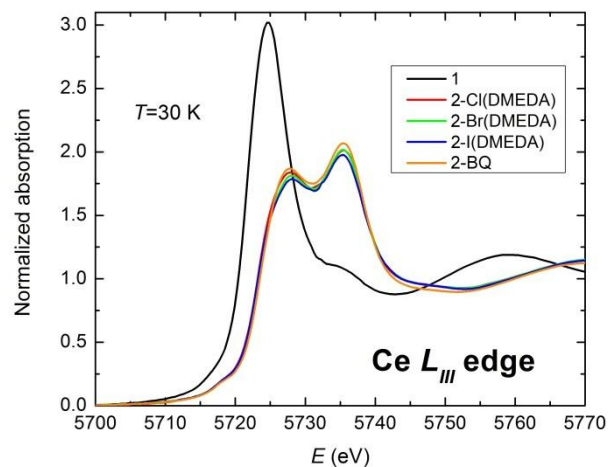

Figure 4. XANES Measurements of **1**, **2–X(DMEDA)**, and **2–BQ**.

Electrochemistry and UV-Vis. Cyclic voltammetry measurements for all of the complexes were conducted in THF using 0.1 M [NPr$_4$][BAr$^F_4$] as the supporting electrolyte. Ce-

rium-based reductions and return oxidation waves were observed for all Ce^{IV}–X compounds, while the extent of electrochemical reversibility differed within the series. Values of $E_{1/2}$ varied with the strength of the donor; a 200 mV range was observed for the series. The relatively small potential range can be rationalized from the relationship of the Ce^{IV}–O$_{BINOLate}$ and Ce^{IV}–X bond distances (Table 1). As the Ce^{IV}–X bond distance becomes shorter, the average Ce^{IV}–O$_{BINOLate}$ distances grow longer, which results in small variations of the total electron density at the Ce^{IV} center.

In contrast, the identity of M$^+$ resulted in a large range of potentials, over 880 mV within the same ligand framework. By decreasing the strength of the O$_{BINOLate}$–M$^+$ interactions more electron density is concentrated closer to the Ce^{IV} center, and shifts the Ce$^{III/IV}$ couple to more negative potentials. Incorporation of Li$^+$ versus Cs$^+$ results in a 400 mV difference in observed potentials. Further tuning of the Ce$^{III/IV}$ couple can be achieved by changing the neutral ligand, which attenuates the Lewis acidity of M$^+$. The presence of a stronger ligand such as 18–crown–6 makes [K$_2$(18–Crown–6)$_2$][(BINOLate)$_3$Ce] (6–Crown) more difficult to reduce than [K$_2$(THF)$_4$(BINOL)][(BINOLate)$_3$Ce] (6–BINOL) by 445 mV. The culmination of all of these effects makes 6–Crown amongst the most negatively shifted Ce$^{III/IV}$ couples reported.[1a,9c,9e,22b]

Compounds 2–X, 4, 6, and 8 are intensely colored purple and red complexes, and show broad absorption features in the visible spectrum that we have assigned as ligand to metal charge transfer (LMCT) bands (Figure 5). The observed values of $1/\lambda_{max}$(LMCT) and $E_{1/2}$ trend to higher energies and more negative potentials with more electron-rich Ce^{IV} centers. With the exception of 2–N$_3$ (for further discussion, see Supporting Information, Figure S47), the inner sphere functionalized products, Ce^{IV}–X, display little variation in $1/\lambda_{max}$(LMCT) and $E_{1/2}$ (Table 2). We postulate that the identity of X is only a minor contributor to the overall electronic environment of the cerium cation, and tentatively assign the LMCT as BINOLate-based in character. Similar to the reduction potentials, the identity of M$^+$ greatly impacts the electronics at Ce^{IV}, where a ~2,500 cm^{-1} blue shift of the LMCT $1/\lambda_{max}$ was observed moving from Li$^+$ to Cs$^+$.

The use of heterobimetallic frameworks allows for a rational modulation of Ce^{IV} electronic properties and should be useful for future redox applications. By increasing the Lewis acidity of the redox-inactive metal less electron density is donated to the Ce^{IV} cation, which shifts the $E_{1/2}$ to more positive potentials and the LMCT to lower energies.

2.4 Inner Sphere Ligand Reorganization in Oxidation Reactions of CeMB (M = Li, Na, K, Cs)

Prior to our studies, quantitative information on the impact of ligand reorganization on cerium(III) oxidation reactions was not available. Given that the choice of M$^+$ determines the reactivity preferences of the CeMB system and effects the ability of the complex to reorganize for substrate binding at the rare earth cation in related REMB complexes,[25,29] we pursued voltammetric and spectroscopic studies to further assess cerium(III) oxidation reaction kinetics.
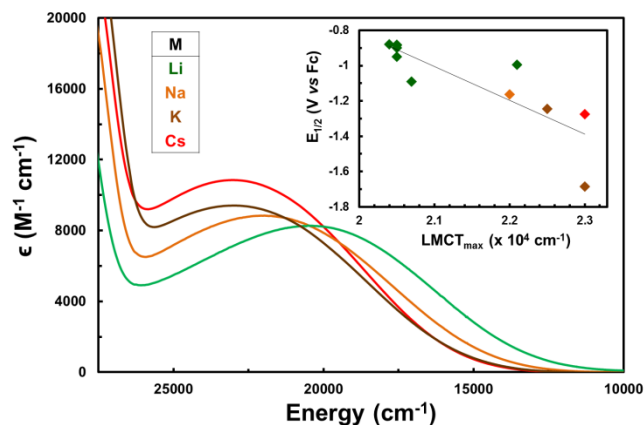

Figure 5. Electronic absorption spectra showing ligand to metal charge transfer (LMCT) absorption features of Ce^{IV}MB, M = Li, Na, K, Cs. 2–Cl (green), 4–BINOL (orange), 6–BINOL (brown), and 8 (red). (*Inset*) Plot of $E_{1/2}$ vs LMCT max for 2, 4, 6, and 8.

Table 1. Electrochemical and UV-Vis data for Ce^{IV}MB

Ce^{IV}MB	LMCT $1/\lambda_{max}$ (x 10^{-4} cm^{-1})	$E_{1/2}$ (V *vs* Fc)^a	Avg. Ce^{IV}–X (Å)	Avg. Ce^{IV}–O$_{BINOLate}$ (Å)
Li 2–Cl	2.05	−0.885	2.667(2)	2.301(6)
Li 2–Cl(DMEDA)	2.05	−0.915	2.7115(7)	2.325(4)
Li 2–Br(DMEDA)	2.05	−0.900	2.896(3)	2.297(9)
Li 2–I(DMEDA)	2.05	−0.950	3.1414(11)	2.294(4)
Li 2–NCS	2.04	−0.880	2.4175(21)	2.284(3)
Li 2–N$_3$	2.21	−0.997	2.353(3)	2.306(3)
Li 2-OAr	2.07	−1.092	2.191(4)	2.319(3)
Na 4–BINOL	2.20	−1.163	---	2.243(12)
K 6–BINOL	2.25	−1.245	---	2.243(3)
K 6–Crown	2.30	−1.685	---	2.240(20)
Cs 8	2.30	−1.275	---	2.201(7)

a – Measured by cyclic voltammetry in THF using a 3 mm diameter glassy carbon working electrode; v = 100 mV/s; [Ce] ≈ 1 mM; [NPr$_4$][BAr$^F_4$] ≈ 100 mM.
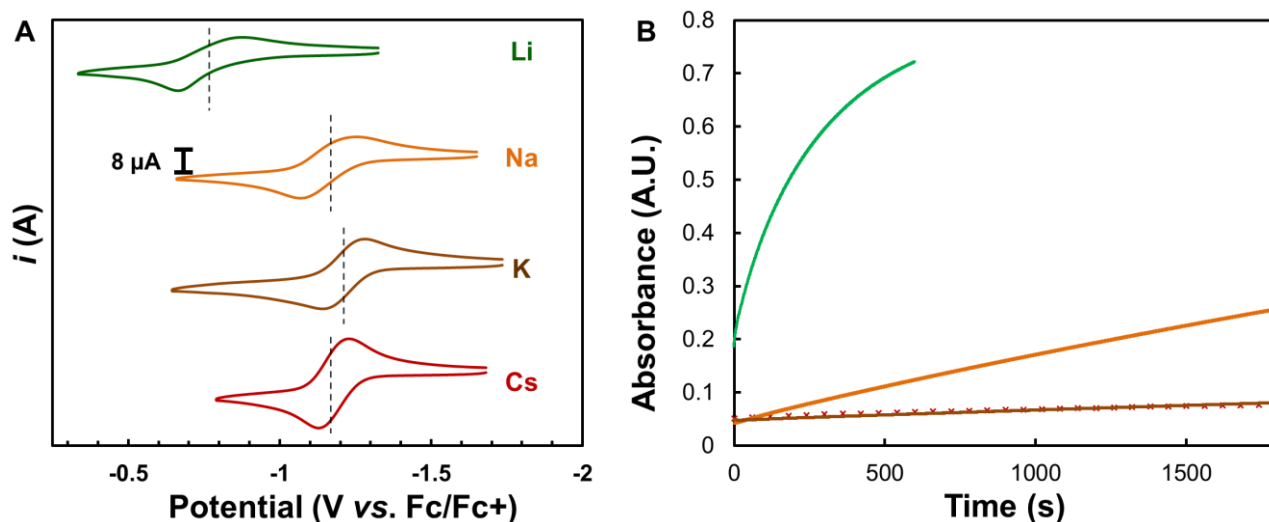
Figure 6. (A) Cyclic voltammograms measured for CeMB (M = Li (**1**), Na (**3**), K (**5**), and Cs (**7**)) in THF:CH$_3$CN (1:6) using a 3 mm diameter glassy carbon working electrode; ν = 50 mV/s; [Ce] ≈ 1mM; [NPr$_4$][BAr$^F_4$] ≈ 0.1 M. Dashed lines drawn to illustrate positions of E$_{1/2}$. (B) Pseudo-first order rate data for **1**, **3**, **5**, and **7** in THF using UV-Vis absorption spectroscopy; [Ce]:[Ph$_3$CCl] = 1:10. **1** (green), **3** (orange), **5** (brown), **7** (red).

Table 2. Electrochemical properties and oxidation kinetics of CeMB.

| Entry	CeMB (M)	E_{pa} (V vs. Fc)^a	E_{pc} (V vs. Fc)^a	ΔE_p (V)^a	k_s (× 10^{-4} cm^2 s^{-1})^{b,c}	Solvent	k_{obs} (× 10^{-4} s^{-1})^d
1	**7** (Cs)	−1.100 (−1.131)	−1.290 (−1.231)	0.190 (0.100)	10.1 (33.2)	THF	0.112
2	**5** (K)	−1.065 (−1.145)	−1.365 (−1.275)	0.300 (0.140)	8.95 (13.8)	THF	0.216
3	**3** (Na)	−0.905 (−1.073)	−1.245 (−1.250)	0.340 (0.180)	6.08 (9.68)	THF	1.93
4	**1** (Li)	−0.475 (−0.665)	−1.065 (−0.875)	0.590 (0.210)	4.34 (5.53)	THF	30.0
5	**1–(DMEDA)** (Li)	−0.565	−1.085	0.520	---	THF	51.7
6	**1** (Li)	---	---	---	---	Tol	150
7	**1** (Li)	---	---	---	---	Tol	5.46 ^{e}

a – Measured by cyclic voltammetry in THF using a 3 mm diameter glassy carbon working electrode; ν = 50 mV/s; [Ce] ≈ 1mM; [NPr$_4$][BAr$^F_4$] ≈ 0.1 M. Values in parentheses were obtained using THF:CH$_3$CN (1:6) instead of THF. b – Calculated using Kochi's method (see Supporting Information).[30] c – Calculated using Nicholson and Shain's and method (see Supporting Information).[31] d –formation under pseudo-first order conditions using UV-Vis absorption spectroscopy;[CeMB] :[Ph$_3$CCl] = 1 : 10. e – 5 equiv of triphenylphosphine oxide (TPPO) added.

Electrochemical Studies of CeMB (M = Li, Na, K, Cs). Electrochemical measurements were performed using cyclic voltammetry of **1**, **3**, **5**, and **7** in THF and THF:CH$_3$CN (1:6) using 0.1 M [NPr$_4$][BAr$^F_4$] (BAr$^F_4$ = tetrakis[3,5-bis(trifluoromethyl)phenyl]borate) as a supporting electrolyte to corroborate trends in solution electrochemical properties and chemical reactivity. Use of THF:CH$_3$CN (1:6) improved solution resistances (≤ 150 Ω) for all CeMB complexes (Figure 3a, Table 2), while preserving their solution structures.

Redox-inactive metal cations play unique roles in the electron transfer processes of biological[11b,32] and model systems,[33] where the Lewis acidity of the cation has been shown to significantly influence the formal potentials and the rates of heterogeneous and homogeneous ET. In the CeMB framework the choice of alkali metal results in an unprecedented 450 mV range for the Ce$^{III/IV}$ couple, which is a greater range than that obtained to date through covalent modifications of a ligand framework.[34]

The rates of electron transfer associated with the Ce$^{III/IV}$ couple were also impacted by the choice of redox-inactive metal, where values of k_s (Table 2) followed k_s(Cs$^+$) > k_s(K$^+$) > k_s(Na$^+$) > k_s(Li$^+$) in both solvent media investigated. Comparison of k_s values where $E_{1/2}$ varies significantly, M = Li versus M = Na, K, Cs, is difficult as the thermodynamic driving force ($\Delta G°$) and reorganization energy (λ) contribute to the overall rate of heterogeneous electron transfer, k_s.[35] For complexes **3**, **5**, and **7**, values of $E_{1/2}$ are basically conserved, so changes in k_s directly reflect differences in reorganization energy of the complexes. Consequently, complex reorganization energy trends followed λ(Na$^+$) > λ(K$^+$) > λ(Cs$^+$), which prompted us to investigate the rates of chemical oxidation with trityl chloride to determine whether ligand reorganization affected chemical reactivity.

Chemical Oxidation Rate Studies. Pseudo-first order rate studies were performed for the oxidation of CeMB with trityl chloride, monitoring the growth of characteristic CT absorption bands centered between 435–487 nm (see the Support-
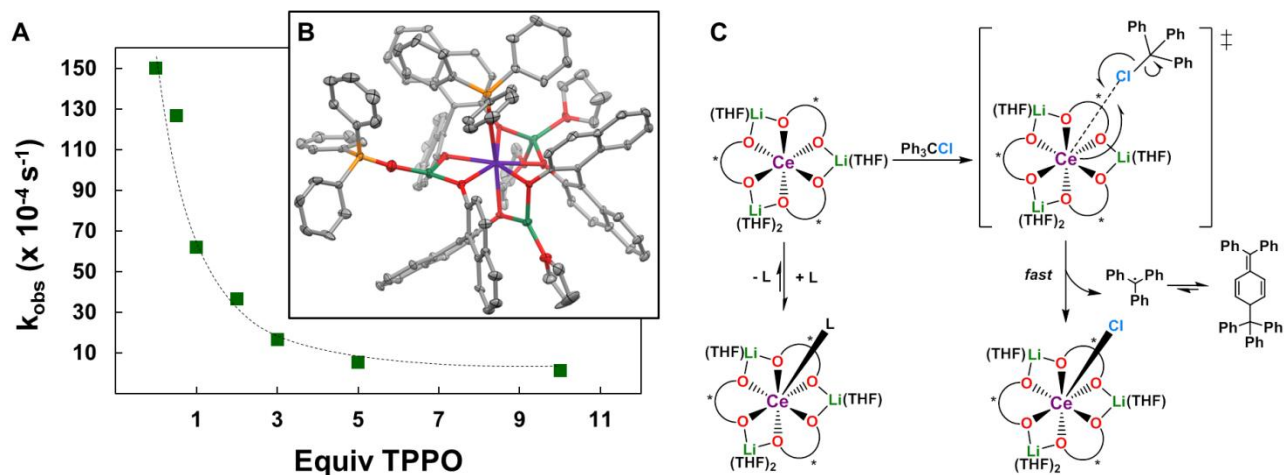
Figure 7. (A) k_{obs} under pseudo-first order kinetics (1:10 [1]:Ph₃CCl) in toluene in the presence of varying equivalents of TPPO (dotted line drawn as a guide for the eye). (B) Thermal ellipsoid plot of **1–2TPPO**, with ellipsoids shown at 30% probability. (C) Proposed inner sphere mechanism for the oxidation of **1** with trityl chloride.

ing Information) by UV-Vis absorption spectroscopy. Reactions were first order in the complexes and trityl chloride, where representative rate data are displayed in Figure 6b. The values of k_{obs} (Table 2) follow $k_{obs}(Cs^+) < k_{obs}(K^+) < k_{obs}(Na^+) << k_{obs}(Li^+)$, and differ by ≥250-fold between **1** and **7** (entries 1–4). This was counter to expectations for an outer sphere mechanism as predicted from the electrochemical measurements, where one would expect k_{obs} to follow $k_{obs}(Cs^+) > k_{obs}(K^+) > k_{obs}(Na^+) > k_{obs}(Li^+)$.

Similar behavior has been observed for reduction of organic substrates with Sm^{II}, where the degree of coordinative saturation at the Sm^{II} ion will direct inner sphere or outer sphere ET processes.[36] For inner sphere processes, coordinative saturation decreases the rate of chemical oxidation to Sm^{III}, and rates do not follow with measured reduction potentials. This behavior is directly comparable to that observed for CeMB; [Li₃(THF)₅][(BINOLate)₃Ce·THF] (**1**) is the weakest reducing agent, but because it has the most accessible Ce^{III} center it undergoes the fastest rate of chemical oxidation. Complex **1** can readily support a seventh ligand at the RE and reorganize between six and seven-coordinate geometries at the cerium cation. Reorganization of the ligand framework to a seven-coordinate Ce^{III} ion when M = Na, K, or Cs is much less favorable, and is consistent with previous binding studies of the REMB framework.[25b-d,29]

N,N′-Dimethylethylenediamine, DMEDA, is a useful mechanistic probe to determine the involvement of Li$^+$ centers of the REMB framework in asymmetric catalysis.[25c,d,37] To probe the role of Li$^+$ in the oxidation of **1**, we subjected [Li₃(DMEDA)₃][(BINOLate)₃Ce] (**1–DMEDA**) to pseudo-first order rate studies (see Supporting Information). Previous studies of the REMB frameworks have revealed that coordination of DMEDA at the Li$^+$ centers improves selectivity for substrate binding over THF by creating a smaller binding pocket at the RE^{III} center.[25c,d] Rate studies of **1–DMEDA** revealed a ~1.6 fold increase in k_{obs} (Table 2, entry 5), which supported the assertion that the Li$^+$ cation directs the ability of the Ce^{III} center to bind Lewis bases.

The rate of an inner sphere ET process should be sensitive to competitive binding of a Lewis base at the Ce^{III} ion. Addition of 5 equiv of TPPO, structurally similar to trityl chloride, resulted in a ~27-fold decrease in k_{obs} relative to the reaction performed in the absence of TPPO (Table 1, entries 6 and 7; Figure 7a).

TPPO and trityl chloride are structurally different than other Lewis bases that have been investigated in solution and solid state binding studies with the REMB framework, and could likely display different coordination preferences.[23b,25c,d,29] Shibasaki and coworkers have found that TPPO and substituted triarylphosphine oxides significantly enhance the stereoselectivity in the REMB catalyzed formation of cyanohydrins[38] and 2,2′-substituted terminal epoxides.[39] Previous mechanistic proposals have invoked coordination of phosphine oxide to the Li$^+$ centers, which prompted us to further investigate reaction of **1** with TPPO to elucidate the binding behavior of TPPO within the REMB framework.

TPPO Binding Studies. Addition of 1 equivalent of TPPO to [Li₃(THF)₅][(BINOLate)₃Ce·THF] (**1**) in THF, followed by layering with pentane afforded [Li₃(THF)₃(TPPO)][(BINOLate)₃Ce(TPPO)] (**1–(TPPO)₂**) as the only crystalline product, instead of the intended 1:1 Ce:TPPO adduct (Figure 7b). A rational synthesis of **1–(TPPO)₂** was readily accomplished by adding 2 equiv of TPPO to **1** in THF, which afforded **1–(TPPO)₂** as light yellow crystals in 83% yield. Interestingly, a 1:1 Ce:TPPO adduct, [Li₃(DME)₃][(BINOLate)₃Ce(TPPO)]·2DME (**1–TPPO**), can be obtained by layering concentrated DME solutions with pentane and can be isolated as light yellow crystals in 82% yield (Figure S32). **1–TPPO** and **1–(TPPO)₂** are the first examples of phosphine oxide coordinated in the REMB framework, and provide direct structural evidence that the central RE^{III} can readily accommodate coordination of phosphine oxides and structurally similar ligands.

Crystals of **1–(TPPO)₂** dissolved in tol–d_8 or THF–d_8 displayed fluxional solution behavior as judged by ^{1}H-, ^{7}Li{^{1}H}-, and ^{31}P{^{1}H}-NMR spectra recorded at 300 K. One ^{7}Li signal

was observed, consistent with 3 chemically equivalent Li ions due to rapid TPPO/THF exchange on the NMR time scale. Two broad ^{31}P signals were observed in a 1:1 ratio representative of slow exchange on the NMR time scale of TPPO bound at the cerium (44 ppm) and lithium (31 ppm) cations (see Supporting Information). Interestingly, the relevant stoichiometry used in reported asymmetric catalysis with the REMB framework, 1 equiv of TPPO to 1 equiv RE, reveals a ^{31}P{^{1}H}-NMR consistent with TPPO bound at the Ce^{III} cation, rather than the Li$^+$ cations.[38-39]

Variable temperature ^{1}H-, ^{7}Li{^{1}H}-, and ^{31}P{^{1}H}-NMR were performed to gain insight and thermodynamic information about the ligand exchange processes. In tol–d_8 at 250 K the solution symmetry of **1–(TPPO)$_2$** agreed with that of the X-ray structure; the ^{7}Li{^{1}H} NMR spectrum revealed three unique signals (Figure S17), and the ^{31}P{^{1}H} spectrum displayed two well-resolved signals. Collection of ^{7}Li{^{1}H}- and ^{31}P{^{1}H}-NMR spectra over the range of 250 K to 325 K (see Supporting Information) allowed for an estimation of the free enthalpy of activation ($\Delta G^{\ddagger}$) for the ligand exchange processes.[40] Barriers obtained for the exchange of TPPO between Li centers and between the Li and Ce centers were 11.4 kcal/mol and 12.6 kcal/mol respectively. These barriers are accessible at room temperature, and corroborate the observed inhibition kinetics upon addition of TPPO; larger amounts of TPPO are needed to maintain coordinative saturation of the Ce^{III} cation, because TPPO exchanges between the multiple Lewis-acid binding sites.

Our proposed mechanism to explain the reactivity of [Li$_3$(THF)$_5$][(BINOLate)$_3$Ce·THF] (**1**) with trityl chloride is shown in Figure 7c. Compound **1** undergoes reversible ligand exchange, where dissociation of neutral ligand at Ce^{III} results in an open coordination site. The rate-determining step is association of trityl chloride to form the transient encounter complex, which undergoes rapid ET to form the oxidatively functionalized product, **2–Cl** and trityl radical. Association of trityl chloride is inhibited by the addition of Lewis bases, like TPPO, which compete for binding at the Ce^{III} center.

3. Conclusions

We have demonstrated that the choice of redox-inactive metal, M, has a dramatic impact on ligand reorganization, which impacts both thermodynamic and kinetic aspects of cerium(III) oxidation reactions. Choice of M facilitates divergent oxidation reactivity utilizing the same ligand framework and oxidant; in the case of M = Li, the first general examples of inner sphere functionalization were achieved through oxidative functionalization and salt-metathesis, whereas M = Na, K, and Cs undergo salt elimination pathways. Our studies offer an alternative and complementary strategy to oxidant-directed product outcomes, and have furnished novel Ce^{IV} complexes in straightforward routes in high yields.

The electronic properties of the Ce^{III} and Ce^{IV} compounds are also readily tuned by the Lewis acidity of M. The most dramatic effects were observed with the Ce^{IV} complexes where the unprecedented range of $E_{1/2}$ (~800 mV) and CT band position (2500 cm^{-1}) highlights the potential of incorporating redox-inactive metals to fine-tune electronic properties at the cerium cation.

Our mechanistic investigations have provided the first quantitative insights into the impact of ligand reorganization on Ce^{III} oxidation reactions. We have found that ligand reorganization is critical to effectively facilitate inner sphere oxidation reactions; [Li$_3$(THF)$_5$][(BINOLate)$_3$Ce·THF] (**1**) undergoes chemical oxidation >250 times faster than [Cs$_6$(THF)$_4$][(μ-BINOLate-κ-1O^1,2O^2)$_2$(BINOLate)$_4$Ce$_2$] (**7**), and is due to the more accessible Ce^{III} cation rather than values of k_s or $E_{1/2}$. Binding studies with triphenylphosphine oxide provide energetic estimates for ligand exchange processes, and further support our proposed inner sphere oxidation mechanism. Furthermore, the TPPO binding studies clarify the role of phosphine oxide in REMB catalyzed asymmetric reactions.

The development of predictable Ce^{III} oxidation chemistry can be readily accomplished through control of ligand reorganization. Heterobimetallic frameworks are beneficial in these regards, and we expect that these findings will contribute to the rational design and synthesis of functionalized cerium platforms for various redox applications. Further studies on ligand dynamics and oxidation pathways in RE redox chemistry are underway.

ASSOCIATED CONTENT

Supporting Information. Experimental details, NMR spectra, electrochemical data, UV-vis data, and crystallographic data (CIF). This material is available free of charge via the Internet at http://pubs.acs.org.

AUTHOR INFORMATION

Corresponding Author

* E-mail: schelter@sas.upenn.edu; pwalsh@sas.upenn.edu

References

(1) (a) Piro, N. A.; Robinson, J. R.; Walsh, P. J.; Schelter, E. J. *Coord. Chem. Rev.* **2013**, in press. (b) Aspinall, H. C. *Chemistry of the f-block Elements*; Overseas Publishing Company: UK, 2001; Vol. 1. (c) Cotton, S. *Lanthanide and Actinide Chemistry*; John Wiley & Sons Ltd: West Sussex, England, 2006.

(2) (a) Molander, G. A. *Chem. Rev.* **1992**, *92*, 29. (b) Nair, V.; Balagopal, L.; Rajan, R.; Mathew, J. *Acc. Chem. Res.* **2004**, *37*, 21. (c) Ho, T. L. *Synthesis* **1973**, 347. (d) Imamoto, T.; Koide, Y.; Hiyama, S. *Chem. Lett.* **1990**, 1445.

(3) (a) Das, A. K. *Coord. Chem. Rev.* **2001**, *213*, 307. (b) Connelly, N. G.; Geiger, W. E. *Chem. Rev.* **1996**, *96*, 877. (c) Rüttinger, W.; Dismukes, G. C. *Chem. Rev.* **1997**, *97*, 1. (d) Fillol, J. L.; Codola, Z.;

Garcia-Bosch, I.; Gomez, L.; Pla, J. J.; Costas, M. *Nat. Chem.* **2011**, *3*, 807. (e) Ellis, W. C.; McDaniel, N. D.; Bernhard, S.; Collins, T. J. *J. Am. Chem. Soc.* **2010**, *132*, 10990. (f) Tagore, R.; Chen, H. Y.; Zhang, H.; Crabtree, R. H.; Brudvig, G. W. *Inorg. Chim. Acta* **2007**, *360*, 2983. (g) Gersten, S. W.; Samuels, G. J.; Meyer, T. J. *J. Am. Chem. Soc.* **1982**, *104*, 4029.

(4) (a) Kreuzer, T.; Lox, E. S.; Lindner, D.; Leyrer, J. *Catal. Today* **1996**, *29*, 17. (b) Inaba, H.; Tagawa, H. *Solid State Ionics* **1996**, *83*, 1. (c) Trovarelli, A. *Catalysis by Ceria and Related Materials*; Imperial College Press: London, 2002. (d) Trovarelli, A.; de Leitenburg, C.; Boaro, M.; Dolcetti, G. *Catal. Today* **1999**, *50*, 353. (e) Trovarelli, A. *Catal. Rev. - Sci. Eng.* **1996**, *38*, 439.

(5) Vivier, L.; Duprez, D. *Chemsuschem* **2010**, *3*, 654.

(6) (a) Farrauto, R. J.; Lampert, J. K.; Hobson, M. C.; Waterman, E. M. *Appl. Catal., B* **1995**, *6*, 263. (b) Shyu, J. Z.; Otto, K.; Watkins, W. L. H.; Graham, G. W.; Belitz, R. K.; Gandhi, H. S. *J. Catal.* **1988**, *114*, 23. (c) Zafiris, G. S.; Gorte, R. J. *J. Catal.* **1993**, *139*, 561.

(7) (a) Murray, E. P.; Tsai, T.; Barnett, S. A. *Nature* **1999**, *400*, 649. (b) Park, S. D.; Vohs, J. M.; Gorte, R. J. *Nature* **2000**, *404*, 265. (c) Shao, Z. P.; Haile, S. M. *Nature* **2004**, *431*, 170. (d) Atkinson, A.; Barnett, S.; Gorte, R. J.; Irvine, J. T. S.; McEvoy, A. J.; Mogensen, M.; Singhal, S. C.; Vohs, J. *Nat. Mater.* **2004**, *3*, 17. (e) Steele, B. C. H. *Solid State Ionics* **2000**, *129*, 95.

(8) (a) Fu, Q.; Saltsburg, H.; Flytzani-Stephanopoulos, M. *Science* **2003**, *301*, 935. (b) Bunluesin, T.; Gorte, R. J.; Graham, G. W. *Appl. Catal., B* **1998**, *15*, 107. (c) Hilaire, S.; Wang, X.; Luo, T.; Gorte, R. J.; Wagner, J. *Appl. Catal., A* **2001**, *215*, 271.

(9) (a) Robinson, J. R.; Carroll, P. J.; Walsh, P. J.; Schelter, E. J. *Angew. Chem., Int. Ed.* **2012**, *51*, 10159. (b) Robinson, J. R.; Booth, C. H.; Carroll, P. J.; Walsh, P. J.; Schelter, E. J. *Chem. Eur. J.* **2013**, *19*, 5996. (c) Williams, U. J.; Mahoney, B. D.; Lewis, A. J.; DeGregorio, P. T.; Carroll, P. J.; Schelter, E. J. *Inorg. Chem.* **2013**, *52*, 4142. (d) Mahoney, B. D.; Piro, N. A.; Carroll, P. J.; Schelter, E. J. *Inorg. Chem.* **2013**. (e) Bogart, J. A.; Lewis, A. J.; Medling, S. A.; Piro, N. A.; Carroll, P. J.; Booth, C. H.; Schelter, E. J. *Inorg. Chem.* **2013**, *52*, 11600.

(10) (a) Morton, C.; Alcock, N. W.; Lees, M. R.; Munslow, I. J.; Sanders, C. J.; Scott, P. *J. Am. Chem. Soc.* **1999**, *121*, 11255. (b) Casely, I. J.; Liddle, S. T.; Blake, A. J.; Wilson, C.; Arnold, P. L. *Chem. Commun.* **2007**, 5037.

(11) (a) Moser, C. C.; Keske, J. M.; Warncke, K.; Farid, R. S.; Dutton, P. L. *Nature* **1992**, *355*, 796. (b) B., G. H.; Winkler, J. R. *Annu. Rev. Biochem.* **1996**, *65*, 537. (c) Gray, H. B.; Malmstrom, B. G.; Williams, R. J. P. *J. Biol. Inorg. Chem.* **2000**, *5*, 551.

(12) (a) Rosokha, S. V.; Kochi, J. K. *J. Org. Chem.* **2002**, *67*, 1727. (b) Rosokha, S. V.; Kochi, J. K. *J. Am. Chem. Soc.* **2007**, *129*, 3683. (c) Rosokha, S. V.; Kochi, J. K. *Acc. Chem. Res.* **2008**, *41*, 641. (d) Bullock, J. P.; Bond, A. M.; Boéré, R. T.; Gietz, T. M.; Roemmele, T. L.; Seagrave, S. D.; Masuda, J. D.; Parvez, M. *J. Am. Chem. Soc.* **2013**, *135*, 11205.

(13) (a) Creutz, C.; Taube, H. *J. Am. Chem. Soc.* **1973**, *95*, 1086. (b) Sutin, N.; Brunschwig, B. S.; Creutz, C.; Winkler, J. R. *Pure Appl. Chem.* **1988**, *60*, 1817. (c) Brunschwig, B. S.; Sutin, N. *Coord. Chem. Rev.* **1999**, *187*, 233. (d) Bosnich, B. *Inorg. Chem.* **1999**, *38*, 2554.

(14) (a) Balzani, V.; Scandola, F.; Orlandi, G.; Sabbatini, N.; Indelli, M. T. *J. Am. Chem. Soc.* **1981**, *103*, 3370. (b) Matsumoto, M.; Kodama, H.; Funahashi, S.; Takagi, H. D. *Inorganic Reaction Mechanisms* **2000**, *2*, 19. (c) Yee, E. L.; Hupp, J. T.; Weaver, M. J. *Inorg. Chem.* **1983**, *22*, 3465.

(15) (a) Hitchcock, P. B.; Hulkes, A. G.; Lappert, M. F. *Inorg. Chem.* **2004**, *43*, 1031. (b) Hitchcock, P. B.; Huang, Q. G.; Lappert, M. F.; Wei, X. H. *J. Mater. Chem.* **2004**, *14*, 3266. (c) Eisenstein, O.; Hitchcock, P. B.; Hulkes, A. G.; Lappert, M. F.; Maron, L. *Chem. Commun.* **2001**, 1560. (d) Crozier, A. R.; Bienfait, A. M.; Maichle-Mossmer, C.; Tornroos, K. W.; Anwander, R. *Chem. Commun.* **2013**, *49*, 87. (e) Droese, P.; Crozier, A. R.; Lashkari, S.; Gottfriedsen, J.; Blaurock, S.; Hrib, C. G.; Maichle-Moessmer, C.; Schaedle, C.; Anwander, R.; Edelmann, F. T. *J. Am. Chem. Soc.* **2010**, *132*, 14046.

(16) Barry, J. E.; Finkelstein, M.; Moore, W. M.; Ross, S. D.; Eberson, L.; Jonsson, L. *J. Org. Chem.* **1982**, *47*, 1292.

(17) Nelson, I. V.; Iwamoto, R. T. *J. Electroanal. Chem. (1959)* **1964**, *7*, 218.

(18) Dröse, P.; Gottfriedsen, J. *Z. Anorg. Allg. Chem.* **2008**, *634*, 87.

(19) (a) Ganesan, V.; Rosokha, S. V.; Kochi, J. K. *J. Am. Chem. Soc.* **2003**, *125*, 2559. (b) Hubig, S. M.; Rathore, R.; Kochi, J. K. *J. Am. Chem. Soc.* **1999**, *121*, 617. (c) Binstead, R. A.; McGuire, M. E.; Dovletoglou, A.; Seok, W. K.; Roecker, L. E.; Meyer, T. J. *J. Am. Chem. Soc.* **1992**, *114*, 173. (d) Lu, K.; Earley, J. E. *Inorg. Chem.* **1993**, *32*, 189. (e) Sun, J.; Stanbury, D. M. *Inorg. Chem.* **1998**, *37*, 1257. (f) Salman, H. M. A.; Mahmoud, M. R.; Abou-El-Wafa, M. H. M.; Rabie, U. M.; Crabtree, R. H. *Inorg. Chem. Commun.* **2004**, *7*, 1209. (g) Thorneley, R. N. F.; Kipling, B.; Sykes, A. G. *J. Chem. Soc. A* **1968**, 2847.

(20) (a) Evans, W. J.; Deming, T. J.; Olofson, J. M.; Ziller, J. W. *Inorg. Chem.* **1989**, *28*, 4027. (b) Suh, S.; Guan, J.; Mîinea, L. A.; Lehn, J.-S. M.; Hoffman, D. M. *Chem. Mater.* **2004**, *16*, 1667.

(21) (a) Ciampolini, M.; Mani, F.; Nardi, N. *J. Chem. Soc., Dalton Trans.* **1977**, 1325. (b) DelaRosa, M.; Bousman, K.; Welch, J.; Toscano, P. *J. Coord. Chem.* **2002**, *55*, 781.

(22) (a) Dröse, P.; Gottfriedsen, J.; Hrib, Cristian G.; Jones, Peter G.; Hilfert, L.; Edelmann, Frank T. *Z. Anorg. Allg. Chem.* **2011**, *637*, 369. (b) Broderick, E. M.; Thuy-Boun, P. S.; Guo, N.; Vogel, C. S.; Sutter, J.; Miller, J. T.; Meyer, K.; Diaconescu, P. L. *Inorg. Chem.* **2011**, *50*, 2870.

(23) (a) Sasai, H.; Suzuki, T.; Itoh, N.; Tanaka, K.; Date, T.; Okamura, K.; Shibasaki, M. *J. Am. Chem. Soc.* **1993**, *115*, 10372. (b) Sasai, H.; Arai, T.; Satow, Y.; Houk, K. N.; Shibasaki, M. *J. Am. Chem. Soc.* **1995**, *117*, 6194.

(24) (a) Mullica, D. F.; Farmer, J. M.; Kautz, J. A. *Inorg. Chem. Commun.* **1998**, *1*, 217. (b) Liu, J.-F.; Xian, H.-D.; Zhao, G.-L. *Acta Crstallogr. Sect. E.-Struct Rep. Online* **2009**, *65*, m650. (c) Shannon, R. D. *Acta Crystallogr. Sec. A* **1976**, *32*, 751.

(25) (a) Aspinall, H. C.; Bickley, J. F.; Dwyer, J. L. M.; Greeves, N.; Kelly, R. V.; Steiner, A. *Organometallics* **2000**, *19*, 5416. (b) Wooten, A. J.; Carroll, P. J.; Walsh, P. J. *Org. Lett.* **2007**, *9*, 3359. (c) Wooten, A. J.; Carroll, P. J.; Walsh, P. J. *Angew Chem Int Edit* **2006**, *45*, 2549. (d) Wooten, A. J.; Carroll, P. J.; Walsh, P. J. *J. Am. Chem. Soc.* **2008**, *130*, 7407.

(26) (a) Caulton, K. G.; Hubert-Pfalzgraf, L. G. *Chem. Rev.* **1990**, *90*, 969. (b) Mehrotra, R. C.; Singh, A.; Tripathi, U. M. *Chem. Rev.* **1991**, *91*, 1287. (c) Evans, W. J.; Sollberger, M. S.; Ziller, J. W. *J. Am. Chem. Soc.* **1993**, *115*, 4120. (d) Schumann, H.; Meese-Marktscheffel, J. A.; Esser, L. *Chem. Rev.* **1995**, *95*, 865. (e) Zimmermann, M.; Anwander, R. *Chem. Rev.* **2010**, *110*, 6194. (f) Mandal, S. K.; Roesky, H. W. *Acc. Chem. Res.* **2009**, *43*, 248. (g) Kempe, R.; Noss, H.; Irrgang, T. *J. Organomet. Chem.* **2002**, *647*, 12.

(27) (a) Kerridge, A.; Coates, R.; Kaltsoyannis, N. *J. Phys. Chem. A* **2009**, *113*, 2896. (b) Ashley, A.; Balazs, G.; Cowley, A.; Green, J.; Booth, C. H.; O'Hare, D. *Chem. Commun.* **2007**, 1515. (c) Streitwieser, A.; Kinsley, S. A.; Jenson, C. H.; Rigsbee, J. T. *Organometallics* **2004**, *23*, 5169. (d) Walter, M. D.; Booth, C. H.; Lukens, W. W.; Andersen, R. A. *Organometallics* **2009**, *28*, 698. (e) Booth, C. H.; Walter, M. D.; Daniel, M.; Lukens, W. W.; Andersen, R. A. *Phys. Rev. Lett.* **2005**, *95*, 267202. (f) Bian, Y.; Jiang, J.; Tao, Y.; Choi, M. T. M.; Li, R.; Ng, A. C. H.; Zhu, P.; Pan, N.; Sun, X.; Arnold, D. P.; Zhou, Z.-Y.; Li, H.-W.; Mak, T. C. W.; Ng, D. K. P. *J. Am. Chem. Soc.* **2003**, *125*, 12257.

(28) Kaindl, G.; Schmiester, G.; Sampathkumaran, E. V.; Wachter, P. *Phys Rev B* **1988**, *38*, 10174.

(29) Di Bari, L.; Lelli, M.; Pintacuda, G.; Pescitelli, G.; Marchetti, F.; Salvadori, P. *J. Am. Chem. Soc.* **2003**, *125*, 5549.

(30) (a) Klingler, R. J.; Kochi, J. K. *J. Am. Chem. Soc.* **1980**, *102*, 4790. (b) Klingler, R. J.; Kochi, J. K. *J. Phys. Chem.* **1981**, *85*, 1731.

(31) (a) Nicholson, R. S.; Shain, I. *Anal. Chem.* **1964**, *36*, 706. (b) Nicholson, R. S. *Anal. Chem.* **1965**, *37*, 1351.

(32) (a) I. Bertini; Gray, H. B.; Lippard, S. J.; Valentine, J. S. *Biological Inorg. Chem.: Structure and Reactivity*; University Science Books: Sausalito, CA, 2007; Vol. 25. (b) *Electron Transfer in Inorganic, Organic, and Biological Systems*; American Chemical Society, 1991; Vol. 228. (c) Eberson, L. E. *Electron Transfer Reactions in Organic Chemistry; Reactivity and Structure*; Springer: Heidelberg, 1987; Vol. 25.

(33) (a) Kanady, J. S.; Mendoza-Cortes, J. L.; Tsui, E. Y.; Nielsen, R. J.; Goddard, W. A.; Agapie, T. *J. Am. Chem. Soc.* **2012**, *135*, 1073. (b) Tsui, E. Y.; Tran, R.; Yano, J.; Agapie, T. *Nat. Chem.* **2013**, *5*, 293. (c) Park, Y. J.; Ziller, J. W.; Borovik, A. S. *J. Am. Chem. Soc.* **2011**, *133*, 9258. (d) Lacy, D. C.; Park, Y. J.; Ziller, J. W.; Yano, J.; Borovik, A. S. *J. Am. Chem. Soc.* **2012**, *134*, 17526. (e) Park, Y. J.; Cook, S. A.; Sickerman, N. S.; Sano, Y.; Ziller, J. W.; Borovik, A. S. *Chem. Sci.* **2013**, *4*, 717. (f) Fukuzumi, S. *Org. Biomol. Chem.* **2003**, *1*, 609. (g) Fukuzumi, S.; Ohkubo, K. *Chem. Eur. J.* **2000**, *6*, 4532. (h) Fukuzumi, S. *Electron Transfer in Chemistry*; Wiley-VCH: Weinheim, 2001. (i) Ohkubo, K.; Menon, S. C.; Orita, A.; Otera, J.; Fukuzumi, S. *J. Org. Chem.* **2003**, *68*, 4720. (j) Fukuzumi, S. In *Prog. Inorg. Chem.*; John Wiley & Sons, Inc.: 2009, p 49. (k) Morimoto, Y.; Kotani, H.; Park, J.; Lee, Y.-M.; Nam, W.; Fukuzumi, S. *J. Am. Chem. Soc.* **2010**, *133*, 403. (l) Fukuzumi, S.; Morimoto, Y.; Kotani, H.; Naumov, P.; Lee, Y. M.; Nam, W. *Nat. Chem.* **2010**, *2*, 756. (m) Fukuzumi, S.; Ohkubo, K. *Coord. Chem. Rev.* **2010**, *254*, 372.

(34) Wester, D. W.; Palenik, G. J.; Palenik, R. C. *Inorg. Chem.* **1985**, *24*, 4435.

(35) (a) Marcus, R. A. *Annu. Rev. Phys. Chem.* **1964**, *15*, 155. (b) Zhu, J.; Wang, J.; Stell, G. *J. Chem. Phys.* **2006**, *125*.

(36) (a) Miller, R. S.; Sealy, J. M.; Shabangi, M.; Kuhlman, M. L.; Fuchs, J. R.; Flowers, R. A. *J. Am. Chem. Soc.* **2000**, *122*, 7718. (b) Prasad, E.; Flowers, R. A. *J. Am. Chem. Soc.* **2002**, *124*, 6895. (c) Prasad, E.; Knettle, B. W.; Flowers, R. A. *J. Am. Chem. Soc.* **2002**, *124*, 14663. (d) Prasad, E.; Knettle, B. W.; Flowers, R. A. *J. Am. Chem. Soc.* **2004**, *126*, 6891. (e) Flowers, I. I. R. *Synlett* **2008**, *2008*, 1427. (f) Sadasivam, D. V.; Teprovich, J. A.; Procter, D. J.; Flowers, R. A. *Org. Lett.* **2010**, *12*, 4140. (g) Enemaerke, R. J.; Daasbjerg, K.; Skrydstrup, T. *Chem. Commun.* **1999**, 343. (h) Enemaerke, R. J.; Hertz, T.; Skrydstrup, T.; Daasbjerg, K. *Chem. Eur. J.* **2000**, *6*, 3747.
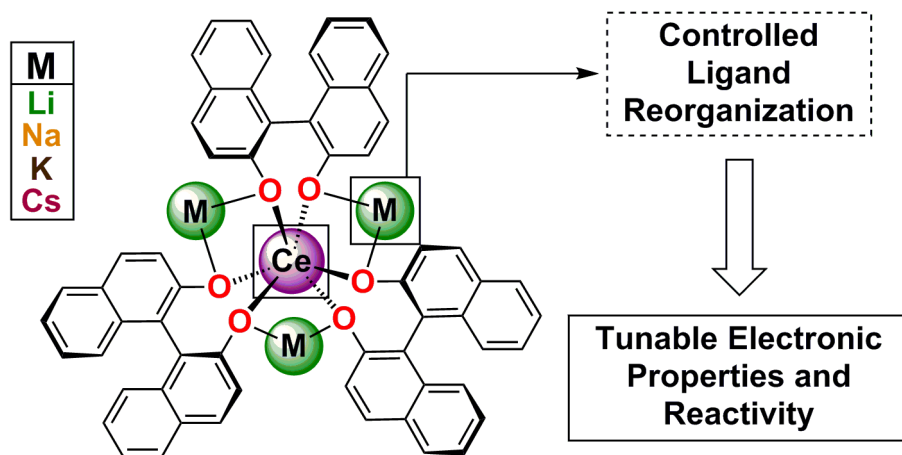
(37) Robinson, J. R.; Carroll, P. J.; Walsh, P. J.; Schelter, E. J. *Organometallics* **2013**, *32*, 1493.

(38) (a) Yamagiwa, N.; Abiko, Y.; Sugita, M.; Tian, J.; Matsunaga, S.; Shibasaki, M. *Tetrahedron: Asymmetry* **2006**, *17*, 566.(b) Yamagiwa, N.; Tian, J.; Matsunaga, S.; Shibasaki, M. *J. Am. Chem. Soc.* **2005**, *127*, 3413. (c) Tian, J.; Yamagiwa, N.; Matsunaga, S.; Shibasaki, M. *Angew. Chem., Int. Ed.* **2002**, *41*, 3636.

(39) (a) Sone, T.; Yamaguchi, A.; Matsunaga, S.; Shibasaki, M. *Molecules* **2012**, *17*, 1617. (b) Sone, T.; Yamaguchi, A.; Matsunaga, S.; Shibasaki, M. *J. Am. Chem. Soc.* **2008**, *130*, 10078.

(40) Friebolin, H. *Basic One- and Two-Dimensional NMR Spectroscopy*; Wiley-VCH, 2005.

Insert Table of Contents artwork here

M
Li
Na
K
Cs

Controlled Ligand Reorganization

Tunable Electronic Properties and Reactivity

DISCLAIMER